Transient Response of Graphite/Epoxy and Kevlar/Epoxy Laminates Subjected to Impact

Douglas S. Cairns* and Paul A. Lagace†
Massachusetts Institute of Technology, Cambridge, Massachusetts

The influence of different parameters on the impact behavior of laminated composite plates is considered analytically. A Rayleigh-Ritz energy method was used to spatially discretize the time-varying boundary value problem and a set of coupled, ordinary differential equations in time were obtained based on the discretized system Lagrangian. The effects of shearing deformation, bending-twisting coupling, and nonlinear contact behavior were included in the model. The resulting equations were integrated using the implicit Newmark beta method without the effects of rotary inertia. The results indicate that the effective mass of the plate is often an important effect in the response to impact events. In general, the influence of the constitutive behavior dominates for very low velocity impact, whereas the target mass properties become more important as the impactor velocity increases. This importance of mass clearly shows that impactor kinetic energy is not sufficient to characterize the impactor as the impactor mass is shown to have a large influence on the resulting dynamic behavior. In addition to these parameters, the effects of preload and material properties are considered and discussed.

Nomenclature

a, b	= in-plane plate dimensions
A_{ij}	= in-plane stiffness
D_{ij}	= bending stiffness
E_{ij}	= extensional modulus of elasticity
G_{ij}	= shear modulus of elasticity
I	= rotary inertia
h	= plate thickness
k	= shearing correction factor
$[K]$	= discretized stiffness matrix
K	= Hertzian spring constant
L	= Lagrangian
$[M]$	= discretized mass matrix
M_{ij}	= applied moments
N_{ij}	= applied in-plane loads
p	= lateral loading
P	= lateral inertia
R	= impactor force
t	= time
T	= kinetic energy
u	= displacement of impactor
U	= strain energy
V	= potential energy
w	= lateral displacement
W	= external energy
x, y	= in-plane coordinates
z	= through-the-thickness coordinate
α	= local indentation
ϵ_{ij}	= extensional strain
γ_{ij}	= shearing strain
κ	= curvature
ν_{ij}	= Poisson's ratio
ψ	= planar rotation
ρ	= mass density
ξ_1, ξ_2	= in-plane location of impact

Received April 12, 1988; presented as Paper 88-2328 at the AIAA/ASME/ASCE/AHS 29th Structures, Structural Dynamics, and Materials Conference, Williamsburg, VA, April 18-20, 1988; revision received Jan. 20, 1989.

*Currently, Research Associate, Hercules Aerospace Company, Magna, Utah.

†Associate Professor, Technology Laboratory for Advanced Composites, Department of Aeronautics and Astronautics. Member AIAA.

I. Introduction

As composite materials continue to be used in aerospace primary structural components, the understanding of the dynamic response of composite structures subjected to impact is necessary for the design and assessment of damage resistance. Impact events may occur in both the manufacturing phase and field use. Typical examples are tool drop and runway kickup. These impact events produce time-varying loads on a structure that can result in compromised properties as a result of damage.

As a first step to understanding the damage resistance issue in composite laminates, an accurate prediction of the transient response during an impact event is necessary. Ideally, simple analytic solutions are desired for understanding this behavior. This would allow the structural analyst to perform parametric studies and establish proper scaling laws. Unfortunately, many features of laminated composite materials preclude simple solutions. Some of these difficulties are outlined here.

Whitney and Pagano[1] showed that the influence of shearing deformation in composite laminates can be significant because of high through-the-thickness shearing compliances. Their results showed that Reissner-Mindlin plate theory, in which planar rotations are introduced as independent variables, can accurately represent the displacement of composite plates compared to exact elasticity solutions. Laterally loaded models that do not account for shearing deformation (i.e., Kirchhoff-Love) can be unrealistically stiff. In impact analyses where contact load introduction is essentially a point load, these errors are severe.

Another complication of laminated composites is the influence of bending-twisting coupling in the constitutive behavior.[2,3] These terms serve to couple modes of vibration such that a simple orthogonal modal superposition method is not valid.

A third, although not severe, complication is the nonlinear constitutive behavior between projectile and target. This behavior is nonlinear[4] and may have hysteresis.[5] This precludes closed-form time convolution of the impact behavior.

The complications introduced by the foregoing factors, as well as other issues, prevent the use of closed-form analyses in determining the time response of composite laminates subjected to impact. Nevertheless, there is a distinct need for a model that is computationally efficient and includes the phenomena just mentioned. Such a model would provide the structural designer with the ability to study the effects of

various parameters on impact and help the designer in determining the most efficient structural configuration. Current models[5-7] generally rely on the finite-element method and may take several hours of CPU time on large computers to analyze one impact scenario.

The objective of the current work is twofold. One is the formulation and implementation of an analytically efficient model that includes the complicating effects which composite laminates possess. This model is meant to allow the structural analyst to make decisions concerning the severity of a given impact event and, furthermore, to provide a framework for the analysis of more complicated structures. The second objective is to use the model to analyze a number of impact events on composite laminates to begin to develop an understanding of the effect of various parameters on the transient response of such plates subjected to impact.

II. Dynamic Model Description

The global model developed for the problem of plates subjected to impact is independent of the details of the local region just beneath the impactor. Only the nature of the local contact behavior is used, and this is determined via an available solution.[4] Thus, the global behavior of the structure is assumed to not be influenced by the local nonlinear behavior except through the nature of the local contact.

An assumed-modes Rayleigh-Ritz energy method to discretize spatial functions is used to solve the time-varying initial problem. This is done since the normal modes of vibration are coupled for anisotropic plates and the forcing function is nonlinear. These difficulties preclude a simple solution of the equations of motion as a simple superposition of modal equations. The spatial functions are discretized to obtain a set of ordinary differential equations in time to be solved. The local contact behavior is assumed to be Hertzian, developing nonlinearities in the forcing function.

The basic problem of a plate subjected to impact from a projectile is shown in Fig. 1. The contact spring is assumed to be Hertzian in nature[4]

$$R = K(\alpha)^{3/2} \tag{1}$$

where R is the force on the plate, α the local indentation, and K a function of the constitutive properties of the indentor and plate. This latter value is obtained from the analysis of Ref. 4.

The bending behavior of the plate is assumed to be anisotropic in that bending-twisting coupling is included. Also, shearing deformation is allowed via the Reissner-Mindlin theory in which planar rotations are introduced as independent variables.[8,9] Under these assumptions, the kinematic relations are

$$\begin{Bmatrix} \kappa_x \\ \kappa_y \\ \kappa_{xy} \end{Bmatrix} = \begin{Bmatrix} \psi_{x,x} \\ \psi_{y,y} \\ \psi_{x,y} + \psi_{y,x} \end{Bmatrix} \tag{2}$$

and

$$\begin{Bmatrix} \gamma_{xz} \\ \gamma_{yz} \end{Bmatrix} = k \begin{Bmatrix} \psi_x - \dfrac{\partial w}{\partial x} \\ \psi_y - \dfrac{\partial w}{\partial y} \end{Bmatrix} \tag{3}$$

where $\{\kappa\}$ are the plate curvatures, $\{\psi\}$ are the planar rotations in Reissner-Mindlin plate theory, γ are the engineering transverse shear strains, k is the shearing correction factor, and w is the lateral displacement. The value of the shearing correction term k used here is the isotropic correction factor of 5/6 shown to be adquate for laminates made from thin plies.[1] The constitutive bending behavior of the plate may be written as

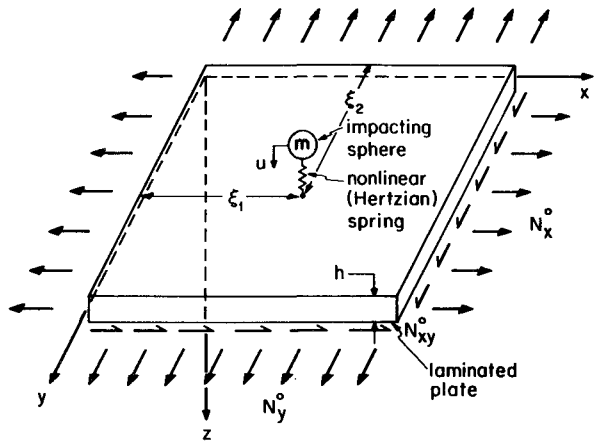

Fig. 1 Sketch of basic problem of plate subjected to impact.

$$\begin{Bmatrix} M_x \\ M_y \\ M_{xy} \end{Bmatrix} = \begin{bmatrix} D_{11} & D_{12} & D_{16} \\ D_{12} & D_{22} & D_{26} \\ D_{16} & D_{26} & D_{66} \end{bmatrix} \begin{Bmatrix} \kappa_x \\ \kappa_y \\ \kappa_{xy} \end{Bmatrix} \tag{4}$$

and

$$\begin{Bmatrix} N_{xz} \\ N_{yz} \end{Bmatrix} = \begin{bmatrix} A_{55} & A_{45} \\ A_{45} & A_{44} \end{bmatrix} \begin{Bmatrix} \gamma_{xz} \\ \gamma_{yz} \end{Bmatrix} \tag{5}$$

where the constitutive properties of interest are defined in the usual manner.[2]

The governing equations of equilibrium will be borne out of the minimization of potential and kinetic energy. For the linear plate assumed, the corresponding bending and shearing strain energies are constructed as surface integrals of the form

$$U_b = \frac{1}{2} \int_0^a \int_0^b \{\kappa\}^T [D] \{\kappa\} \, dy \, dx \tag{6}$$

and

$$U_s = \frac{1}{2} \int_0^a \int_0^b k\{\gamma\}^T [A] \{\gamma\} \, dy \, dx \tag{7}$$

In addition to the strain energy of the laminate, the work associated with the applied loads must be determined. The external work on the plates is the sum of the lateral loading work on the plate and the effect of the midplane loads (in an average sense). These are expressed as W_1 for the lateral work

$$W_1 = -\int_0^a \int_0^b p(x, y) \, w(x, y) \, dy \, dx \tag{8}$$

and as W_n for the in-plane loads

$$W_n = \frac{1}{2} \int_0^a \int_0^b \begin{Bmatrix} w_{,x} \\ w_{,y} \end{Bmatrix}^T \begin{bmatrix} N_x^0 & N_{xy}^0 \\ N_{xy}^0 & N_y^0 \end{bmatrix} \begin{Bmatrix} w_{,x} \\ w_{,y} \end{Bmatrix} dy \, dx \tag{9}$$

In these, $p(x, y)$ is the lateral loading on the plate, $w(x, y)$ the lateral displacement, and N_x^0, N_y^0, and N_{xy}^0 the average in-plane loadings. The corresponding plate kinetic energies are expressed as the surface integrals of the associated mass and velocities

$$T_p = \frac{1}{2} \int_0^a \int_0^b \begin{Bmatrix} \dot{\psi}_x \\ \dot{\psi}_y \\ \dot{w} \end{Bmatrix}^T \begin{bmatrix} I & 0 & 0 \\ 0 & I & 0 \\ 0 & 0 & P \end{bmatrix} \begin{Bmatrix} \dot{\psi}_x \\ \dot{\psi}_y \\ \dot{w} \end{Bmatrix} dy \, dx \tag{10}$$

where $(\dot{o})$ denotes a derivative with respect to time, and the plate lateral inertia matrix P and plate rotary inertia matrix I are defined via

$$[P, I] = \rho \int_{-h/2}^{+h/2} [1, z^2]\, dz \tag{11}$$

In this latter equation, h is the plate thickness and ρ the mass density of the plate.

In the Rayleigh-Ritz technique, assumed displacement mode shapes are used to transform the spatially continuous system to a discrete system of modal amplitudes.[10] Minimization of the plate potential and kinetic energies results in the governing equation of motion in terms of the transformed system of modal amplitudes. For the spatial discretization of the x and y functions, the displacements are assumed to be separable in x and y. This leads to the following assumed forms for the planar rotations and lateral displacements:

$$\psi_x = \sum A_i(t)\, f_i(x)\, g_i(y) \tag{12}$$

$$\psi_y = \sum B_i(t)\, h_i(x)\, l_i(y) \tag{13}$$

$$w = \sum C_i(t)\, m_i(x)\, n_i(y) \tag{14}$$

where $A_i(t)$, $B_i(t)$, and $C_i(t)$ are the time-varying modal amplitudes and i represents and the $m$nth mode. The mode shapes utilized are expanded as vectors to clearly show the influence of bending-twisting coupling that is an important consideration in dynamic problems.[11] The validity of this approach, with respect to the separability of the functions, has been demonstrated by Wang.[3] Beam functions satisfying the associated displacement boundary conditions are employed to satisfy these conditions.[12,13] In addition, the functions for the planar rotations are derivatives of the lateral displacements in accordance with

$$f_i(x) = m_i'(x) \tag{15a}$$

$$h_i(x) = m_i(x) \tag{15b}$$

$$g_i(y) = n_i(y) \tag{15c}$$

$$l_i(y) = n_i'(y) \tag{15d}$$

where $(\ )'$ denotes a spatial derivative. This choice of functions is particularly appropriate since in the limit as the plate thickness approaches zero, the slope of the lateral displacement can approach the planar rotations, which results in the recovery of Kirchhoff plate theory. This precludes the shear locking problems associated with other types of discretization such as the finite-element method.[14]

Taking V as the potential energy of the plate and T as the kinetic energy of the system, the Lagrangian or action integral is defined as T minus V.[10] Consequently, using the principle of virtual work and then integrate the parts, the governing equations of motion of the plate in terms of modal amplitudes are

$$\frac{d}{dt}\left[\frac{\partial L}{\partial \dot{x}_i}\right] - \frac{\partial L}{\partial x_i} = R_i \tag{16}$$

where x_i is the generalized modal amplitude and R_i the modal forcing amplitude. The Lagrangian equations of motion are developed by placing Eqs. (6-10) into Eq. (16)

$$\begin{bmatrix} I_x & 0 & 0 \\ 0 & I_y & 0 \\ 0 & 0 & M \end{bmatrix} \begin{Bmatrix} \ddot{A}_i \\ \ddot{B}_i \\ \ddot{C}_i \end{Bmatrix} \begin{bmatrix} K_{aa} & K_{ab} & K_{ac} \\ K_{ab} & K_{bb} & K_{bc} \\ K_{ac} & K_{bc} & K_{cc} \end{bmatrix} \begin{Bmatrix} A_i \\ B_i \\ C_i \end{Bmatrix} \begin{Bmatrix} R_{ai} \\ R_{bi} \\ R_{ci} \end{Bmatrix} \tag{17}$$

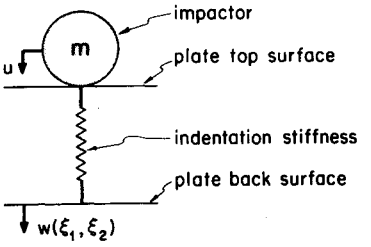

Fig. 2 Local schematic of impacting mass.

The components of the foregoing stiffness matrices are determined by integrating the assumed spatial dependence of modes over the surface. The integrals involving trigonometric functions are evaluated numerically using a ten-point Simpson's rule.[14] This method was chosen since it is more reasonable than other techniques such as Gaussian quadrature,[14] which was developed specifically for functions involving simple polynomials.

It is important to note the presence of the D_{16} and D_{26} coupling terms in the stiffness matrices. These terms provide coupling between the beam functions. If the plate is orthotropic with these terms equal to zero, the orthogonality of the beam functions decouples the modes, resulting in diagonal matrices. This coupling converts a problem that is nearly analytic into one that is far more computationally intensive. If the modes are decoupled, a series of decoupled one-dimensional superposition integrals in time may be performed instead of the matrix equations developed from this coupling.

The schematic of the impacting mass at the local level is shown in Fig. 2. The approach between the two bodies (local indentation) is defined as

$$\alpha(t) = u(t) - w(t, \xi_1, \xi_2) \tag{18}$$

where u is the displacement of the impactor and w the plate displacement due to the global deflection. Utilizing Eq. (1), the particle equation of equilibrium for the ball, equal to the force on the plate, is

$$m\ddot{u} = K(\alpha)^{3/2} = R \tag{19}$$

where m is the impactor mass and R the reaction of the ball.

The external work due to lateral loading was previously defined in Eq. (8). In the present analysis, the plate is assumed to be laterally loaded at the point of contact. This point loading may be considered a Dirac delta function of amplitude R. Therefore, upon integration, the terms are picked-out, as in

$$R_{ci} = R m_i(\xi_i)\, n_i(\xi_2) \tag{20}$$

since these attain values only at the point of impact, ξ_1 and ξ_2. The task of solving Eq. (17) remains.

III. Solution of Equations

Before proceeding with the solution, the system of equations is simplified by statically condensing out the rotary inertia terms. The rotary inertia is the inertia associated with the planar rotations and contributes to the formation of shearing waves in the laminate, whereas the lateral inertia governs the formation of bending waves in the laminate. Several authors[5,6,9] have argued that for the geometries of interest, the rotary inertia terms are small and may be neglected. Indeed, an examination of the relative amplitudes of the mass matrix as defined in Eq. (11) shows that the relative amplitude of the mass matrices (rotary/lateral) is $h^2/12$. For a practical laminate thickness on the order of 1 to 10 mm, this ratio is on the order of 10^{-7} to 10^{-5}. Since the terms populating the matrices are greater in the shearing stiffness matrices than the bending

stiffness matrices, this huge difference in mass illustrates that the frequency arising from the rotary inertia is much higher than that of the lateral displacement. Consequently, static condensation of the system of equations, neglecting the rotary inertia terms, while retaining the influence of shearing deformation, results in

$$[M]\{\ddot{C}_i\}+[K_{cc}^*]\{C_i\}=\{R_{ci}\} \tag{21}$$

where

$$[K_{cc}^*]=\left[K_{cc}-\begin{Bmatrix}K_{ac}\\K_{bc}\end{Bmatrix}^T\begin{bmatrix}K_{aa}&K_{ab}\\K_{ba}&K_{bb}\end{bmatrix}^{-1}\begin{Bmatrix}K_{ac}\\K_{bc}\end{Bmatrix}\right] \tag{22}$$

is the condensed stiffness matrix neglecting rotary inertia. With this manipulation, the equations are in their final form.

Many solution techniques are available for systems of the form of Eqs. (16) and (17). In the present analysis, the Newmark implicit integration scheme (also known as the Newmark beta method) is used.[14] This method is chosen since it is easily implemented and unconditionally stable. However, it can also yield inaccurate results if improper time steps are used. Consequently, caution must be exercised in choosing the time step. Using a time step of 0.1 divided by the highest natural frequency of the reduced problem gives good results. Implementing the general scheme as a constant average-acceleration method (trapezoidal rule with β equal to 1/4), the stepwise equations of motion are

$$\left[M+\frac{(\Delta t)^2}{4}K_{cc}^*\right]\begin{Bmatrix}\ddot{C}_i\\ \ddot{u}\end{Bmatrix}_j=\begin{Bmatrix}R_{ci}\\ R\end{Bmatrix}_j-\frac{(\Delta t)^2}{4}\left[K_{cc}^*\right]\begin{Bmatrix}\ddot{C}_i\\ \ddot{u}\end{Bmatrix}_{j-1}-\Delta t\left[K_{cc}^*\right]\begin{Bmatrix}\dot{C}_i\\ \dot{u}\end{Bmatrix}_{j-1}-\left[K_{cc}^*\right]\begin{Bmatrix}C_i\\ u\end{Bmatrix}_{j-1} \tag{23}$$

with the associated time derivative vectors at the jth time step being

$$\begin{Bmatrix}\dot{C}_i\\ \dot{u}\end{Bmatrix}_j=\begin{Bmatrix}\dot{C}_i\\ \dot{u}\end{Bmatrix}_{j-1}+\frac{\Delta t}{2}\left(\begin{Bmatrix}\ddot{C}_i\\ \ddot{u}\end{Bmatrix}_{j-1}+\begin{Bmatrix}\ddot{C}_i\\ \ddot{u}\end{Bmatrix}_j\right) \tag{24}$$

and

$$\begin{Bmatrix}C_i\\ u\end{Bmatrix}_j=\begin{Bmatrix}C_i\\ u\end{Bmatrix}_{j-1}+\frac{\Delta t}{2}\left(\begin{Bmatrix}\dot{C}_i\\ \dot{u}\end{Bmatrix}_{j-1}+\begin{Bmatrix}\dot{C}_i\\ \dot{u}\end{Bmatrix}_j\right) \tag{25}$$

In these equations, Δt is the incremental time step.

Since the forcing function R is nonlinear, each of the foregoing equations is solved twice at each time increment using the previous forcing term R_{j-1} in a form of predictor-corrector scheme in order to increase accuracy. Also, if the approach, as defined in Eq. (18), is negative, the forcing function R is set to zero and the equations of the impactor and plate decouple (i.e., free vibration). That is, the plate and ball are no longer in contact.

IV. Implementation

The analysis was implemented in FORTRAN 77. Depending on the number of modes required, the analysis may be run on a personal computer. Up to 9 modes in each of the x and y directions fit into 500 kbytes of available computer storage. More modes require a larger computer, but the 9 by 9 mode case was found to be adequate for all applications for the geometries studied. However, the question of the influence of the number of modes utilized should be further investigated, especially for very high-frequency responses. All of the matrix inversion required static condensation of the rotary inertia, and the Newmark implicit integration scheme is self-contained using Gaussian elimination.

The inputs to the problem are the plate constitutive properties, Hertzian spring constant, mass density of the plate, boundary conditions of the plate, initial velocity of the impactor, and mass of the impactor. An eigenvalue subroutine is implemented to determine the highest natural frequency of the plate to determine the time step to be used. This may be overridden to specify any time step desired. The code runs in approximately 4 min of CPU time on a DEC μ-VAX II and approximately 1.5 h of CPU time on an IBM-PC personal computer for 900 time steps. Storage requirements of 250 kbytes are required for storage of the output data.

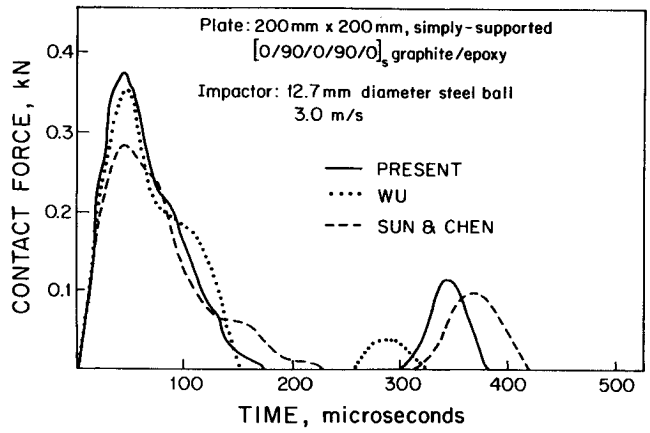

Fig. 3 Contact force vs time for impact of simply supported [0/90/0/90/0]$_s$ T300/934 graphite/epoxy plate.

It is noted that the present analysis requires only a few minutes of CPU time to solve the problem on a DEC VAX 780 computer compared to the several hours of CPU time that may be required for finite-element models on the same computer.[6] This makes the present analysis useful for parametric studies of impact kinetics.

V. Numerical Example

The case of a 200 mm by 200 mm T300/934 graphite/epoxy plate in a [90/0/90/0/90]$_s$ configuration is analyzed. Results for this particular configuration are available in the literature[6,7] and the present results are compared to these. The constitutive properties utilized for the basic T300/934 ply are

$$E_{11}=141.2\text{ GPa},\quad E_{22}=9.72\text{ GPa}$$

$$\nu_{12}=0.30,\quad \nu_{23}=0.30$$

$$G_{12}=5.53\text{ GPa},\quad G_{23}=3.74\text{ GPa}$$

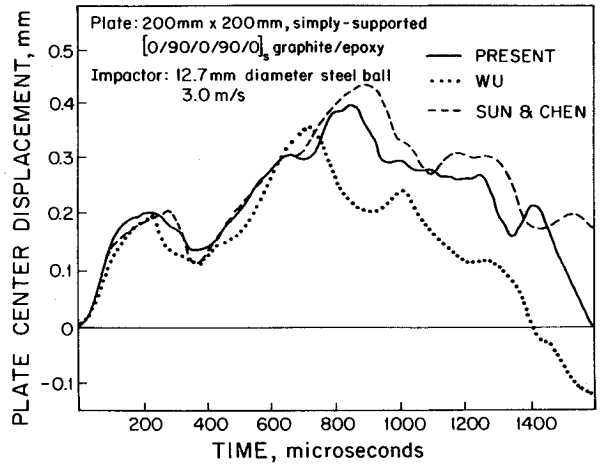

Fig. 4 Center displacement vs time for impact of simply supported [0/90/0/90/0]$_s$ T300/934 graphite/epoxy plate.

with a mass density of 1536 kg/m^3 and a per ply thickness of 0.269 mm. The impactor considered is a 12.7 mm diameter steel sphere at a velocity of 3 m/s. This corresponds to 0.0378 J of initial impactor kinetic energy.

The results of impact force vs time are shown in Fig. 3 along with the results of Wu[6] and Sun and Chen.[7] These authors used finite-element models to obtain solutions. The plate center displacement vs time results are found in Fig. 4. These results have been verified experimentally by Sun and Chen with good correlation. All three analyses yield similar results with the first impact in good agreement with the results of Wu. However, the analyses of Wu, and Sun and Chen also incorporate a modified Hertzian contact spring that accounts for some permanent deformation. This may explain the slightly higher impact loads predicted for the second impactor contact. In general, the results predicted here are close to those obtained by Sun and Chen. This is not surprising since both methods use the same kinematic assumptions. Only the manner in which the problem is discretized is different.

It should be noted that these results are for relatively low-energy (0.03784 J) and velocity (3 m/s) impactor events.

VI. Parametric Analyses

With the viability of the current model established and its relative efficiency, a number of configurations were analyzed to discern the relative influence of various parameters on the transient response of composite plates subjected to impact. For this section, the baseline laminate is "constructed" from Hercules AS4/3501-6 graphite/epoxy with the following constitutive properties:

$$E_{11} = 142.0 \text{ GPa}, \quad E_{22} = 9.81 \text{ GPa}$$

$$\nu_{12} = 0.30, \quad \nu_{23} = 0.34$$

$$G_{12} = 6.0 \text{ GPa}, \quad G_{23} = 3.77 \text{ GPa}$$

The mass density of this material is 1540 kg/m^3 and the per ply thickness is 0.134 mm. The basic configuration considered is a 190 mm by 70 mm plate with a $[\pm 45/0]_{2s}$ layup. The baseline impact event is caused by a steel ball of 12.7 mm diameter, with the base case being at a velocity of 44 m/s corresponding to an energy level of 8 J.

The force vs time history for a clamped-free plate (indicating the conditions along the x axis/y axis) for this baseline case is shown in Fig. 5. This is the case of a wide beam. An important factor in examining this and other results is the peak impact loads. It has been proposed that these peak impact loads are the controlling influence in the creation of damage in the impact event.[6,15] These peak impact loads are thus a main basis for comparison in addition to the entire impact signature.

Boundary Conditions

A number of cases were run with different boundary conditions. The greatest difference from the baseline case is a clamped-clamped plate. The results for contact force vs time are shown in Fig. 6. In comparing this to the baseline clamped-free case of Fig. 5, the impact signatures are clearly different. However, the peak impact loads are not significantly different (approximately 4.1 kN in the baseline case to 3.7 kN in the current case).

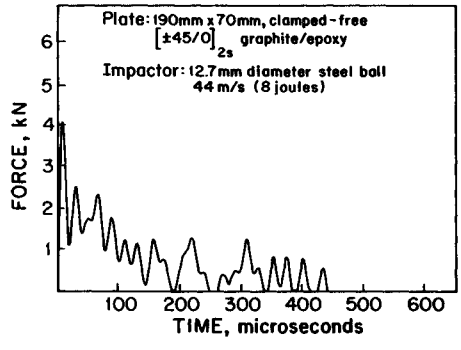

Fig. 5 Contact force vs time for 44 m/s steel ball impact of clamped-free $[\pm 45/0]_{2s}$ AS4/3501-6 graphite/epoxy plate.

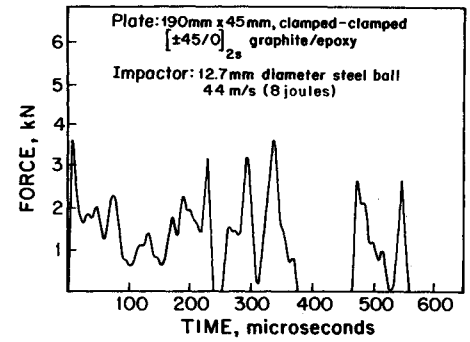

Fig. 6 Contact force vs time for 44 m/s steel ball impact of clamped-clamped $[\pm 45/0]_{2s}$ AS4/3501-6 graphite/epoxy plate.

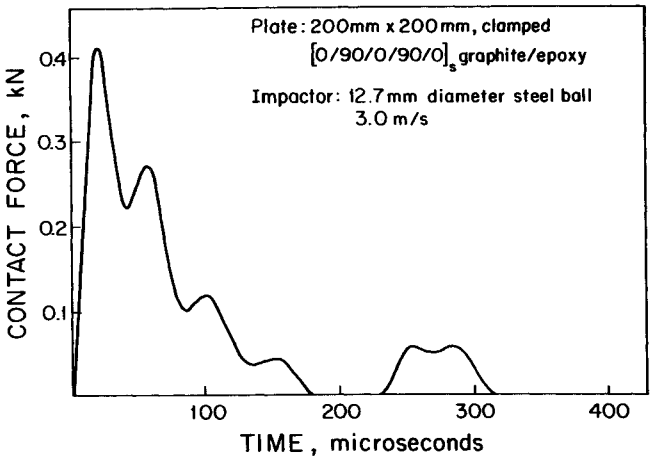

Fig. 7 Contact force vs time for impact of clamped $[0/90/0/90/0]_s$ T300/934 graphite/epoxy plate.

These peak loads are nearly the same for these higher velocity impacts since the response is mass-dominated rather than stiffness-dominated. This explains why the first peak in the clamped-clamped condition is, in fact, slightly lower than in the clamped-free condition as the wide beam has greater lateral inertia. However, the stiffness is important in the remainder of the response as can clearly be seen. This is due to the fact that the different modes of vibration of the plate become important as time progresses.

The effect of boundary conditions was further discerned by analyzing the $[0/90/0/90/0]_s$ graphite/epoxy case, of the previous section, with clamped-clamped conditions, and the force vs time results are presented in Fig. 7. This is compared with the simply-supported case with the results previously presented in Fig. 3. The loads for the clamped case are slightly higher than in the simply-supported case, showing the influence of static stiffness. Here, the stiffer plate has higher impact loads at this very low-velocity impact. However, the peak impact loads are not significantly different (on the order of 10%). This again indicates the importance of the effective mass properties and the result that boundary conditions can have little influence on the peak impact loads in this regime. It is important to note that the impactor mass is also low in all these cases.

Impactor Mass

The importance of the mass and relative inertias is further illustrated when considering the effect of the impactor mass.

The impact force vs time history for an acrylic impactor with an initial velocity of 82 m/s (giving an impact energy of 4 J) on the baseline $[\pm 45/0]_{2s}$ graphite/epoxy laminate is shown in Fig. 8. The acrylic impactor has a mass 0.14 times that of the steel impactor.

For the case of the acrylic impactor, the impact is more severe in terms of the peak impactor force in comparison to the force vs time history of the steel impactor at twice the energy level (see Fig. 5). The acrylic impactor creates a peak impact force of 4.8 kN, as opposed to 4.1 kN in the steel case at twice the impactor energy level. Analysis of a steel impactor at 4 J of impactor energy yields a peak impact load of 2.8 kN. Furthermore, the duration of the impact event in the case of the acrylic impactor is much shorter as the ball is reflected in a shorter time because of its lower inertia.

The increase in peak impact force may be explained by the fact that the plate, having inertia, cannot respond quickly in a global manner to the incoming projectile. This allows the impactor traveling at a higher velocity to indent into the laminate to a greater extent at the local level, thus producing higher-impact loads prior to the lateral deflection of the plate.

These results clearly show that the practice of describing an impact event by the impactor energy is insufficient. Since the relative inertias (as well as stiffnesses) of the impactor and target are so important in the dynamic response, both the mass and velocity, and thus the energy, of the impactor must be specified. A local contact event is governed by the frequency of the ball oscillating on the plate, via the contact stiffness, whereas a structural impact event is governed by the fundamental frequency of the structure. In most actual cases, these two base responses interact and all the parameters must therefore be specified.

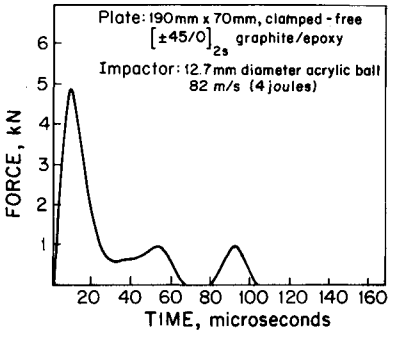

Fig. 8 Contact force vs time for 82 m/s acrylic ball impact of clamped-free $[\pm 45/0]_{2s}$ AS4/3501-6 graphite/epoxy plate.

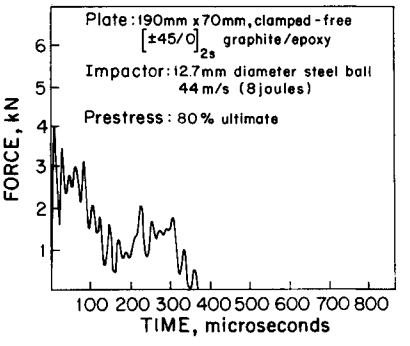

Fig. 9 Contact force vs time for 44 m/s steel ball impact of clamped-free $[\pm 45/0]_{2s}$ AS4/3501-6 graphite/epoxy plate with preload.

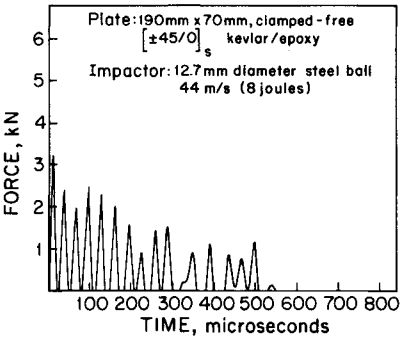

Fig. 10 Contact force vs time for 44 m/s steel ball impact of clamped-free $[\pm 45/0]_{2s}$ Kevlar/epoxy plate.

Preload

The effect of a tensile preload on the response of the plate was also considered. The impact load vs time history for a $[\pm 45/0]_{2s}$ graphite/epoxy laminate under a tensile preload of 700 MPa (corresponding to 80% of the virgin ultimate stress of 876 MPa) using a steel impactor at 44 m/s (8 J of impactor energy) is shown in Fig. 9. Again, comparing the first peak load in this figure to that for the baseline case, of Fig. 5, with no preload, shows that the tensile preload has virtually no influence on the resulting peak impact load for these velocity impacts. This is similar to the findings of Sun and Chen.[7] However, the impact signature has changed and the influence of higher modes is clearly seen.

The fact that there is little effect on the peak impact load can again be attributed to the fact that the event is mass-dominated, whereas the in-plane preload serves to increase the *in situ* stiffness of the plate. This latter effect is the reason for the difference in the overall impact signature. This effect was further illustrated in the results for center deflection (not shown here), where the in-plane preload limits the center deflection to one-third of the value seen in the baseline case.

Material Type

One other composite material was considered in this investigation. This material is Kevlar/epoxy (SP328) with the following basic ply properties:

$$E_{11} = 63.7 \text{ GPa}, \quad E_{22} = 5.03 \text{ GPa}$$

$$\nu_{12} = 0.28, \quad \nu_{23} = 0.34$$

$$G_{12} = 4.03 \text{ GPa}, \quad G_{23} = 1.67 \text{ GPa}$$

with a mass density of 1347 kg/m^3 and a per ply thickness of 0.207 mm. Since there is a ply thickness difference between this material and the baseline graphite/epoxy, a similar, but not the same, laminate was considered for the Kevlar/epoxy case: $[\pm 45/0]_s$. This has the same ply orientations, but only 6 plies as compared to 12 in the graphite/epoxy case. Its thickness is approximately 20% less than the baseline $[\pm 45/0]_{2s}$ graphite/epoxy configuration.

Nevertheless, important conclusions can be drawn by comparing the results for contact force vs time, shown in Fig. 10, with those of the baseline case (Fig. 5). It is clear that not only is the impact signature quite different with many "restrikes" in the Kevlar/epoxy case, but the peak impact load is significantly lower (3.2 kN compared to 4.1 kN). The reasons for this are threefold. One, the bending stiffnesses of the $[\pm 45/0]_s$ plate are much lower than the baseline graphite/epoxy case due to the lower stiffness of the material. A lower bending stiffness tends to result in lower impact loads since the plate can absorb more of the energy of the impact by global bending and shearing. Two and more important, the Kevlar/epoxy plate has a lower mass than the baseline graphite/epoxy case. This lower lateral inertia results in the acceleration of the plate away from, and releasing contact with, the impactor several times in a more dramatic manner than in the graphite/epoxy laminates. Three, the Kevlar/epoxy has a lower contact stiffness than the graphite (1.259 GN/m$^{1.5}$ compared to 1.729

$GN/m^{1.5}$ for the configurations considered) due to the lower transverse stiffness of the Kevlar/epoxy. This serves to lower the transient loads, especially in the first impact peak where the transverse deflection of the plate is low due to inertia.

VII. Summary

An efficient model has been developed to study the dynamic behavior of composite laminates subjected to impact. The model is able to handle analyses in a fraction of the time necessary for similar analyses utilizing finite elements. With this model, parametric analyses of the transient response were conducted. From the results, a number of important points were demonstrated.

The loads created during impact consist of both contact loads and inertial loads as a result of acceleration of the structure from the impact event. Since the deflections of the plate are quite low during the impact event, the global stiffness and, hence, boundary conditions are found to have little influence on the relatively low impactor masses and relatively high velocities used in this study. In fact, contrary to intuition, the more compliant plates (with respect to the boundary conditions) had greater predicted impact loads in one case because the overall structure is more massive with respect to global deformation. If the impact event (at a given kinetic energy) results from a very high mass and correspondingly low velocity, the influence of the boundary conditions is quite different since the event is dominated by the global behavior of the structure. The dominance of inertia is again evident in laminates under a tensile preload. Even though the global stiffness of the laminate is higher because of the stiffening effects of the preload, the mass properties that dominate the problem for the velocities considered in this study remain unchanged. However, the global behavior and influence of higher modes are more evident.

Since the problem studied here is so dependent on the dynamics of the system, it is strongly dependent on the mass of the constituents. Therefore, the mass of the impactor at a fixed-impact kinetic energy has a strong influence on the impact event as a result of the relative inertia of the projectile and target. Even though the contact stiffness of the lower-mass acrylic impactor vs the steel impactor is lower, the resulting impact forces are higher. Thus, the impact event for a lower-mass, higher-velocity projectile is found to produce greater loads. Again, the argument of the influence of local and global behavior applies. For impact events in which the dynamics of the problem are not a consideration, these arguments may be moot and a completely static model may be applicable.

The dominance of the mass of the constituents was again demonstrated in considering the material of the target plate. The Kevlar/epoxy laminate exhibited lower contact forces due to its lower mass and thus lower inertia. In addition, the lower bending stiffness allows greater acceleration away from the incoming impactor, which also helps to reduce the contact forces. The lower transverse stiffness of the Kevlar/epoxy is also a factor in reducing these contact forces.

These specific conclusions about the effect of various parameters lead to two generic conclusions as to the treatment of the impact event and associated dynamic response. First, using either a local contact model, where the influence of the structural behavior is neglected, or solely a global model, where the local contact behavior is neglected, would be meaningless for impact events that have an equal contribution from the local and global structural level. This is an important conclusion since it means that the use of models that do not consider the effects of each influence is inapplicable in this region. Thus, it is necessary to treat the problem at both the local and global level. Second, both the mass and velocity of the impactor are important. It is therefore insufficient to define the impact solely by the initial impactor energy.

The development of this model allows for the necessary parametric studies of the dynamic behavior, which is not simply a function of one parameter such as impactor energy, global bending, or local contact stiffness. The method employed here is computationally efficient and may be applied to more complex structures, and thus helps in determining scale-up factors, if the vibrational mode shapes are known *a priori*. This method of separation of the local and contact behavior and structural modal behavior holds promise for the practical treatment of determining the damage produced in laminated composite materials subjected to impact when used in conjunction with models to determine local strain fields once the contact loads have been determined.[15]

Acknowledgments

The authors wish to acknowledge the assistance of Professor John Dugundji of MIT's Department of Aeronautics and Astronautics in the development of the analytical technique presented here. The support for this work was provided by a joint Federal Aviation Administration/Navy program under contract N0019-85-C-0090.

References

[1]Whitney, J. M. and Pagano, N. J., "Shear Deformation in Heterogeneous Anisotropic Plates," *Journal of Applied Mechanics,* Vol. 37, 1970, pp. 1031–1036.

[2]Jones, R. M., *Mechanics of Composite Materials,* Scripta, Washington, DC, 1975.

[3]Wang, J. T., "On the Solution of Plates and Composite Materials," *Journal of Composite Materials*, Vol. 2, July 1969, pp. 590–592.

[4]Cairns, D. S. and Lagace, P. A., "Thick Composite Plates Subjected to Lateral Loading," *Journal of Applied Mechanics*, Vol. 54, Sept. 1987, pp. 611–616.

[5]Tan, T. M. and Sun, C. T., "Use of Statical Indentation Laws for the Impact of Composite Plates," *Journal of Applied Mechanics*, Vol. 52, March 1985, pp. 693–698.

[6]Wu, H. Y., "Impact Damage of Composite," Ph.D. Thesis, Dept. of Aeronautics and Astronautics, Stanford Univ., Stanford, CA, 1986.

[7]Sun, C. T. and Chen, J. K. "On the Impact of Initially Stressed Composite Laminates," *Journal of Composite Materials*, Vol. 19, Nov. 1985, pp. 490–504.

[8]Reissner, E., "The Effect of Transverse Shear Deformation on the Bending of Elastic Plates," *Journal of Applied Mechanics*, Vol. 18, June 1945, pp. 67–69.

[9]Mindlin, R. D., "The Effect of Rotary Inertia and Shear on Flexural Motions of Isotropic Elastic Plates," *Journal of Applied Mechanics*, Vol. 18, March 1951, pp. 31–38.

[10]Langhaar, H. L., *Energy Methods in Applied Mechanics*, Wiley, New York, 1962.

[11]Jensen, D. W., Crawley, E. F., and Dugundji, J., "Vibration of Cantilevered Graphite/Epoxy Plates with Bending/Torsion Coupling," *Journal of Fiber Reinforced Plastics and Composites*, Vol. 1, July 1982, pp. 254–269.

[12]Leissa, A. W., "Buckling of Laminated Composite Plates and Shell Panels," U.S. Air Force Wright Aeronautical Lab., Dayton, OH, AFWAL-TR-85-3069, 1985.

[13]Young, D. and Felgar, R. P., "Table of Charateristic Functions Representing the Normal Modes of Vibration of a Beam," Pub. 4913, Bureau of Engineering Research, Univ. of Texas, Austin, TX, 1949.

[14]Bathe, K. J., *Finite Element Procedures in Engineering Analysis*, Prentice-Hall, Englewood Cliffs, NJ, 1982.

[15]Cairns, D. S., "Impact and Post-Impact Response of Graphite/Epoxy and Kevlar/Epoxy Structures, TELAC Rept. 87-15, Massachusetts Institute of Technology, Cambridge, MA, Aug. 1987.